Polymer Chemistry

Accepted Manuscript

This is an *Accepted Manuscript*, which has been through the Royal Society of Chemistry peer review process and has been accepted for publication.

Accepted Manuscripts are published online shortly after acceptance, before technical editing, formatting and proof reading. Using this free service, authors can make their results available to the community, in citable form, before we publish the edited article. We will replace this *Accepted Manuscript* with the edited and formatted *Advance Article* as soon as it is available.

You can find more information about *Accepted Manuscripts* in the Information for Authors.

Please note that technical editing may introduce minor changes to the text and/or graphics, which may alter content. The journal's standard Terms & Conditions and the Ethical guidelines still apply. In no event shall the Royal Society of Chemistry be held responsible for any errors or omissions in this *Accepted Manuscript* or any consequences arising from the use of any information it contains.

ROYAL SOCIETY OF CHEMISTRY

www.rsc.org/polymers

Polymer Chemistry

ARTICLE

Chemotherapeutic copolymers prepared via the RAFT polymerization of prodrug monomers

Received 00th January 20xx,
Accepted 00th January 20xx

DOI: 10.1039/x0xx00000x

www.rsc.org/

H.N. Son[‡,a], S. Srinivasan[‡,a], J.Y. Yhee[b], D. Das[a], B.K. Daugherty[a], G.Y. Berguig[a], V.G. Oehle[c], S.H. Kim[b], K. Kim[b], I.C. Kwon[b,d], P.S. Stayton[a,*], and A.J. Convertine[a,*]

Reversible addition-fragmentation chain transfer (RAFT) polymerization was employed to prepare prodrug polymer carrier systems with the chemotherapeutic agent camptothecin (Cam) and the kinase inhibitor dasatinib (Dt). Copolymers were prepared as dense polyethylene glycol brushes via direct copolymerization of the prodrug macromonomers with polyethylene glycol methacrylate (O950, FW ~ 950 daltons). The brushes display controlled drug release profiles with little burst or late-phase release aberrations. Hydrolysis studies of the hydrophilic copolymers conducted in human serum showed 33 ± 1.7 and 22 ± 2.4 % drug release over the course of 144 h for the ester linked Dt and Cam respectively. Polymer morphology was also shown to play a key role in drug release rates. Copolymers with the drug distributed in the copolymer segment showed faster release rates than diblock copolymers where the hydrophobic drug molecules were localized in discreet hydrophobic blocks. The latter materials were shown to self-assemble into polymeric micelles with the drug block separated from the aqueous phase. Live animal imaging in PC-3 (human prostate cancer cell line) tumor xenographs showed that the fluorescently labeled copolymer brushes were trafficked to the tumor 24 hours post injection. *Ex vivo* analysis of the harvested tissues showed that polymer accumulated in the tumor with kidney excretion. In vitro cytotoxicity measurements conducted in K562-S and K562-R cells demonstrated ability of the macromolecular conjugates to release active drugs. The direct copolymerization of different drug classes into controlled copolymers via RAFT, together with their favorable release profiles, suggest these carriers merit further study as therapeutic systems.

.

A Introduction

Antineoplastic agents often have low therapeutic windows that limit the maximum dose of the drug that may be administered.[1] The toxicities observed for these agents often result from an inability to achieve therapeutic concentrations at the target site and nonspecific cytotoxicity to critical tissues (e.g. bone marrow, renal, cardiac).[2] These drugs may also suffer from low solubility in aqueous media necessitating the use of surfactants and other excipients that may produce additional deleterious effects.[3] Liposomes, which consist of an aqueous volume entrapped by one or more bilayers of lipids, have been developed to enhance the effectiveness of chemotherapeutic agents.[4] These structures allow drugs with varying lipophilicities to be encapsulated within the inner aqueous space or entrapped within the phospholipid bilayer. Sequestration of the chemotherapeutic agents into liposomes not only act as formulation aids but also alters the biodistribution of the drugs allowing a greater fraction of the administered drug to reach the target sites. For example, randomized controlled studies with liposomes encapsulating doxororubicin demonstrated efficacy comparable to that of free doxorubicin, but with significantly less cardiotoxicity.[5]

Despite these advantages liposomes also suffer from a number of limitations including drug leakage and the need for complex formulation processes.[6] As an alternative system with its own advantages and disadvantages, polymer-drug conjugates have been developed in which antineoplstic agents are covalently conjugated to hydrophilic polymer scaffolds. Conjugation of poorly soluble drugs to hydrophilic polymers can increase the solubility and stability of the parent drug while also enhancing the circulation half-lives and reducing immunogenicity. [7,8 9]

[a] *Molecular Engineering and Sciences Institute, department of BioEngineering, Box 355061, Seattle WA, 98195, USA. E-Mail: aconv@uw.edu; Tel: (206) 817 6011.* [‡] *Equally contributing co-first authors*

[b] *Department of Chemical Engineering, University of Seoul, Seoul 130-743, Republic of Korea.*

[c] *Fred Hutchinson Cancer Research Center 1100 Fairview Ave., N., D5-100 Seattle, WA 98109*

[d] *KU-KIST Graduate School, Korea University, Seoul 136-791, Republic of Korea.*

† Electronic Supplementary Information (ESI) available:
See DOI: 10.1039/x0xx00000x

A variety of polymers derived from natural sources (e.g. albumin, chitosan, and heparin) have been employed in FDA-approved nanomedicines.[10] Synthetic nanomedicines based on hydrophilic copolymers such as polyethylene glycol (PEG) and poly(2-hydroxypropyl methacrylamide) (HPMA) have also been developed. [11-14] For example Kopeček et al. have synthesized biodegradable HPMA-epirubicin conjugates for the treatment of ovarian cancer.[15] These conjugates were shown to provide complete tumor remission and long-term inhibition of tumorigenesis in mice bearing human ovarian carcinoma A2780 xenografts.

Davis and coworkers have developed nanoparticulate conjugates of Cam and a cyclodextrin-based polymer (CRLX101). [16,17, 18] In this system Cam is linked covalently to the polymer via a glycine linker to form a hydrolytically cleavable ester bond. In vivo studies have shown that CRLX101 increases the aqueous solubility of Cam by three orders of magnitude and prevents drug degradation via lactone hydrolysis. In another polymer chemistry development, asymmetric bifunctional silyl ether prodrugs of several potent chemotherapeutic agents including Cam, gemcitabine, and Dt were integrated into 200 nm × 200 nm PRINT nanoparticles.[19] The resultant nanoparticles were able to release the active drug with controlled and tunable rates.

Atom transfer radical polymerization (ATRP) and reversible addition-fragmentation chain-transfer (RAFT) polymerization have greatly simplified the synthesis of homogenous polymers with controlled spatially defined functional groups for drug delivery applications.[20-22] These approaches and key historical work have relied largely on post-polymerization conjugation strategies. For example, Emrick and coworkers synthesized polymer drug conjugates by a combination of ATRP and "click" chemistry.[23] In these studies telechelic Cam conjugates were prepared by acylation of camptothecin with bromoisobutyryl bromide to yield the corresponding ATRP initiator. Subsequent polymerization with methacryloyloxyethyl phosphorylcholine yielded a zwitterionic polymer with a single drug moiety at the alpha chain end. The authors also employed a one-pot ATRP-"click" conjugation strategy to prepare graft copolymers with up to 14 % Cam with excellent aqueous solubility.[23] Polymeric prodrugs derived from advanced polymer architectures have also been demonstrated. [24-29] Macrocyclic "Sunflower" polymers incorporating hydrazone-linked doxorubicin and folate targeting ligands were synthesized using a combination of ATRP and "click" chemistry.[24] Recently we employed a similar hydrazone-based strategy to link doxorubicin to antibody-targeted single polymer nanoparticles. The resultant materials were able to incorporate up to 385 drugs per polymer while remaining readily soluble in water.[30]

Macromolecular prodrugs have also been prepared via the controlled polymerization of therapeutic agents that have been reversibly modified with suitable vinyl functionality. This approach is advantageous in that it allows one or more drug moieties to be formulated into the final polymer at predetermined ratios without the need for additional conjugation and purification steps. Direct polymerization of prodrug monomers also enables the therapeutic agent(s) to be placed in discrete block copolymer segments providing additional control over the final morphology as well as control of drug release rates. Zelikin et al. have employed the polymerizable prodrug strategy to prepare ribavirin-based therapeutics for the treatment of human immunodeficiency virus (HIV) and hepatitis C virus (HCV). [31,32] Recently, we reported the use of RAFT polymerization to produce well-defined polymeric prodrugs of Ciprofloxacin, an antibiotic used to treat many Gram negative bacteria, from monomeric drug precursors.[33] Herein we detail the development of macromolecular prodrug therapeutics for cancer therapy derived from the chemotherapeutic agents Cam and Dt using this polymerizable prodrug strategy.

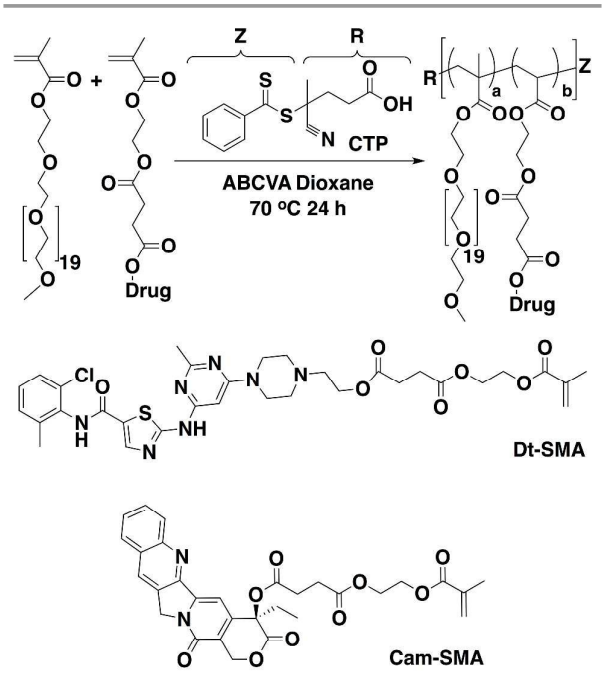

Scheme 1. Synthetic scheme for the preparation of macromolecular prodrugs via (co) polymerization of prodrug monomers with O950.

B Results and Discussion

Synthesis of hydrophilic macromolecular prodrugs

Shown in Scheme 1 are the chemical structures of methacrylate-based prodrug monomers for the tyrosine kinase inhibitor Dt (Dt-SMA) and the topoisomerase I antagonist Cam (Cam-SMA). In this scheme a large O950 (FW ~ 950 Da) comonomer is employed in order to provide a hydrophilic and biocompatible scaffold to which hydrophobic drug molecules can be linked.[34] Previously we have shown that these materials remain biocompatible even at polymer concentration of 300 mg/kg and provide extended circulation times relative to shorter PEG macromonomers.[35] The use of the large PEG

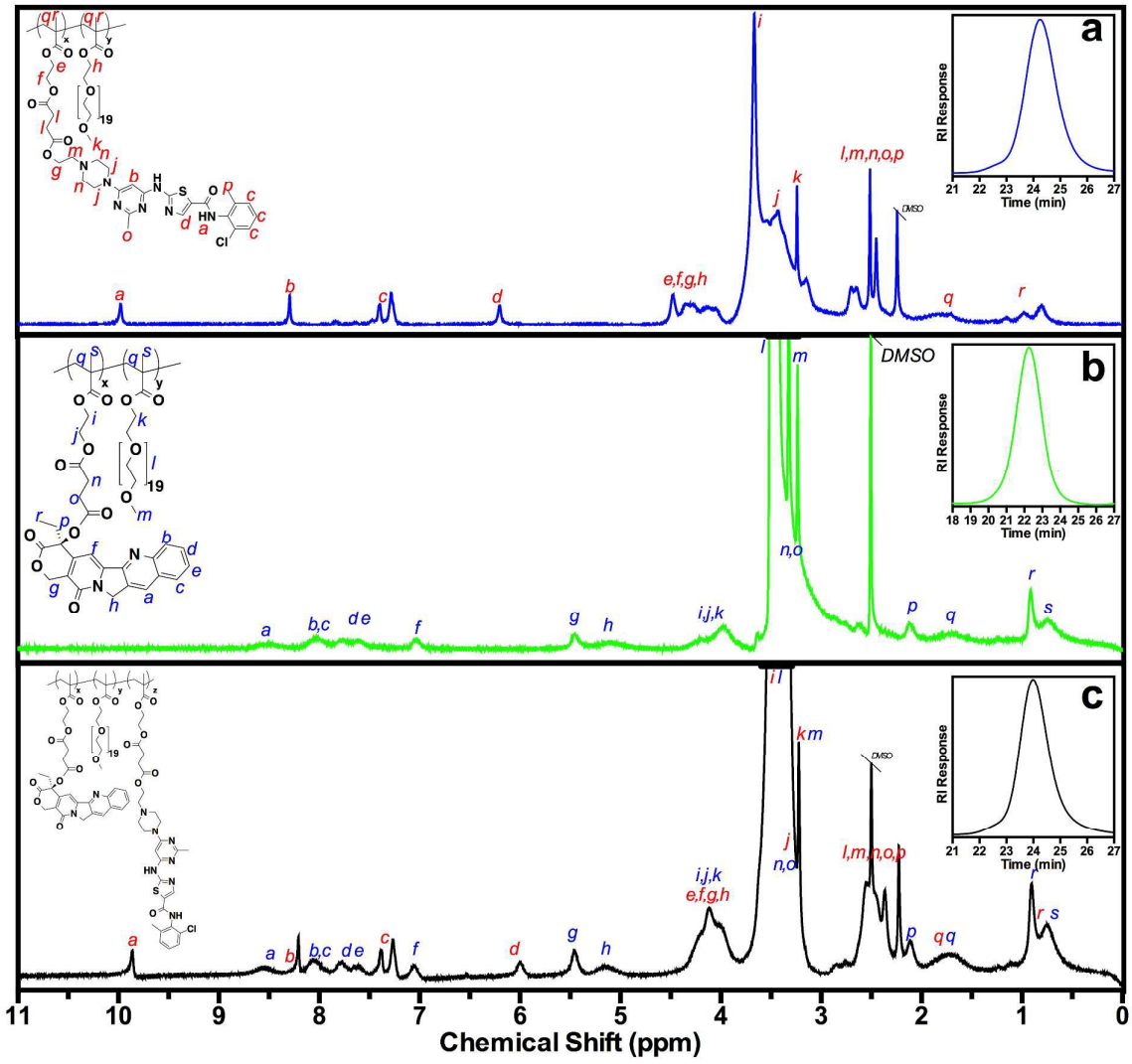

Fig. 1. ^{1}H NMR spectra and molecular weight distributions for poly(Cam-SMA-co-O950), poly(Dt-SMA-co-O950), and poly(Cam-SMA-co-O950-co-Dt-SMA). Absolute Molecular weights were determined using a Wyatt Technology miniDAWN TREOS, 3 angle MALS light scattering instrument and Optilab TrEX, refractive index detector.

macromonomer also allows for polymers with appreciable molecular weights (M_n 5-50 kDa) to be prepared while keeping the overall degree of polymerization low. This provides a mechanism by which the ester-linked side chains connecting the oligoethylene glycol segments to the polymer backbone can ultimately be degraded in vivo to yield low molecular weight fragments that can be eliminated from circulation. Both prodrug monomers are prepared by conjugation of the carboxylic acid-functional methacrylate monomer SMA to hydroxyl residues present on the chemotherapeutic agents. The use of SMA instead of a smaller carboxylic acid monomer (e.g. methacrylic acid) yields prodrug monomers where the sterically bulky drug moieties are separated from the polymer backbone by a small spacer, which may improve copolymerization behavior with the methacrylate-based O950 macromonomer. This spacer also provides two additional ester groups that can be hydrolyzed to liberate the covalently linked drug moieties from the polymer backbone. Copolymerizations of the prodrug monomers with O950 were conducted in DMSO at 70 ^{o}C with CTP and 4,4'-azobis(4-cyanovaleric acid) (ABCVA) as the RAFT chain transfer agent and radical initiator respectively.[36]

Shown in Fig. 1a-c are the ^{1}H NMR spectra and SEC chromatograms for copolymers of Dt-SMA and Cam-SMA with O950 as well as a mixture of both prodrug monomers with O950. For both the poly(Dt-SMA-co-O950) (Fig. 1a) and poly(Cam-SMA-co-O950) (Fig. 1b) copolymers an equimolar initial feed ratio of prodrug monomer to O950 was employed resulting in 47 and 54 mol % of the respective prodrug

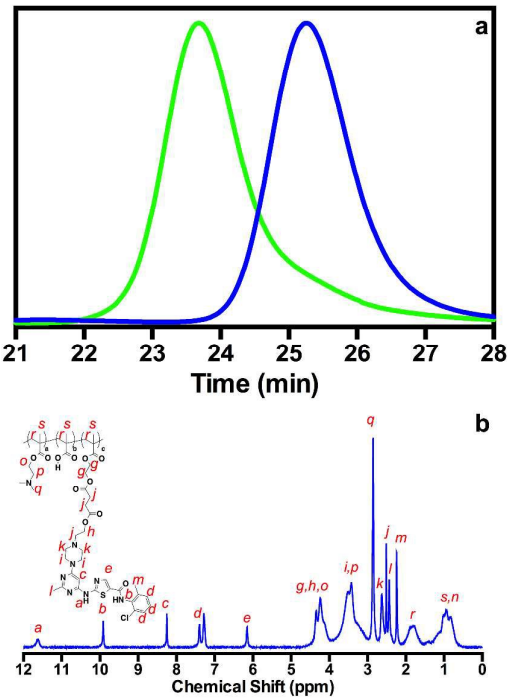

Fig. 2 a. Molecular weight distributions for a poly(tBMA-co-DMAEMA) macroCTA and the corresponding poly[(tBMA-co-DMAEMA)-b-Dt-SMA) diblock copolymer providing evidence for the formation of diblock copolymers. b. ^{1}H NMR spectrum in DMSO-d_6 for the deprotected poly[(MA-co-DMAEMA)-b-Dt-SMA) showing complete removal of the tert-butyl ester protecting groups. Absolute Molecular weights were determined using a Wyatt Technology miniDAWN TREOS, 3 angle MALS light scattering instrument and Optilab TrEX, refractive index detector.

residues in the final copolymers. This feed ratio corresponds to approximately 21.3 and 32.5 wt. % of Cam and Dt drugs in the final copolymers respectively. As can be seen in Fig. 1, all spectra show an intense resonance at around 3.5 ppm that is associated with the 19 ethylene oxide resonances present on O950. Also visible are resonances associated with each of the prodrug monomers.

Following copolymerization, a significant broadening of the comonomer resonances can be seen in ^{1}H NMR spectra for both poly(Cam-SMA-co-O950) and poly(Dt-SMA-co-O950). This result coupled with the lack of vinyl resonances supports the formation of the copolymers with drug compositions that are controllable based on initial monomer stoichiometry. The conditions employed in these studies were also shown to provide copolymers with narrow molecular weight distributions (Fig. 1a-c inserts) with final molecular weights and molar mass dispersities of 26.5 kDa/1.16 and 28.0 kDa/1.10 for poly(Cam-SMA-co-O950) and poly(Dt-SMA-co-O950) respectively. The ability to prepare copolymers with multiple chemotherapeutic agents incorporated into individual polymer chains at predetermined compositions was demonstrated by preparing a copolymer consisting of 24 % Cam-SMA, 27 % Dt-SMA, and 49 mol % O950 (molar feed ratio

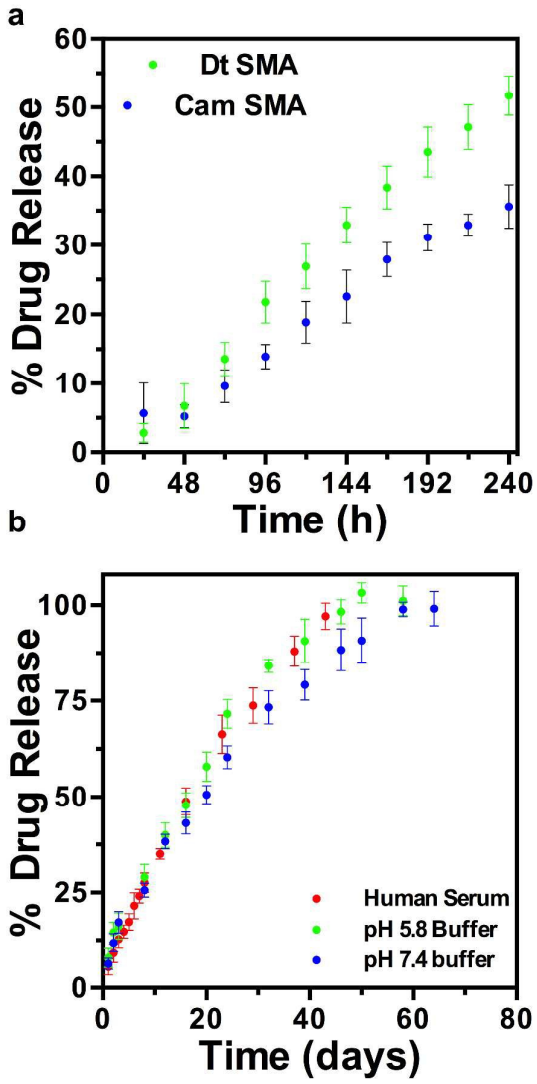

Fig. 3 Drug release as a function of incubation time in human serum at 37 ^{o}C. a. prodrug macromonomers of Cam and Dt b. Drug release as a function of incubation time in buffer and human serum for poly[(DMAEMA-co-MA)-b-(Dt-SMA)].

= 25:25:50). As can be seen in Fig. 1c, the ^{1}H NMR spectrum contains key resonances associated with both prodrug monomers as well as the hydrophilic O950 comonomer. Similar to polymerizations containing a single prodrug monomer the molecular weight distribution remains narrow and symmetric without the appearance of significant high molecular weight coupling or tailing.

Synthesis of poly[(tBMA-co-DMAEMA)-b-(Dt-SMA)]

In order to evaluate the effect of polymer morphology under aqueous conditions on the observed rate of drug release (vide infra) a diblock copolymer, where the hydrophobic drug residues are segregated in a discrete block copolymer segment

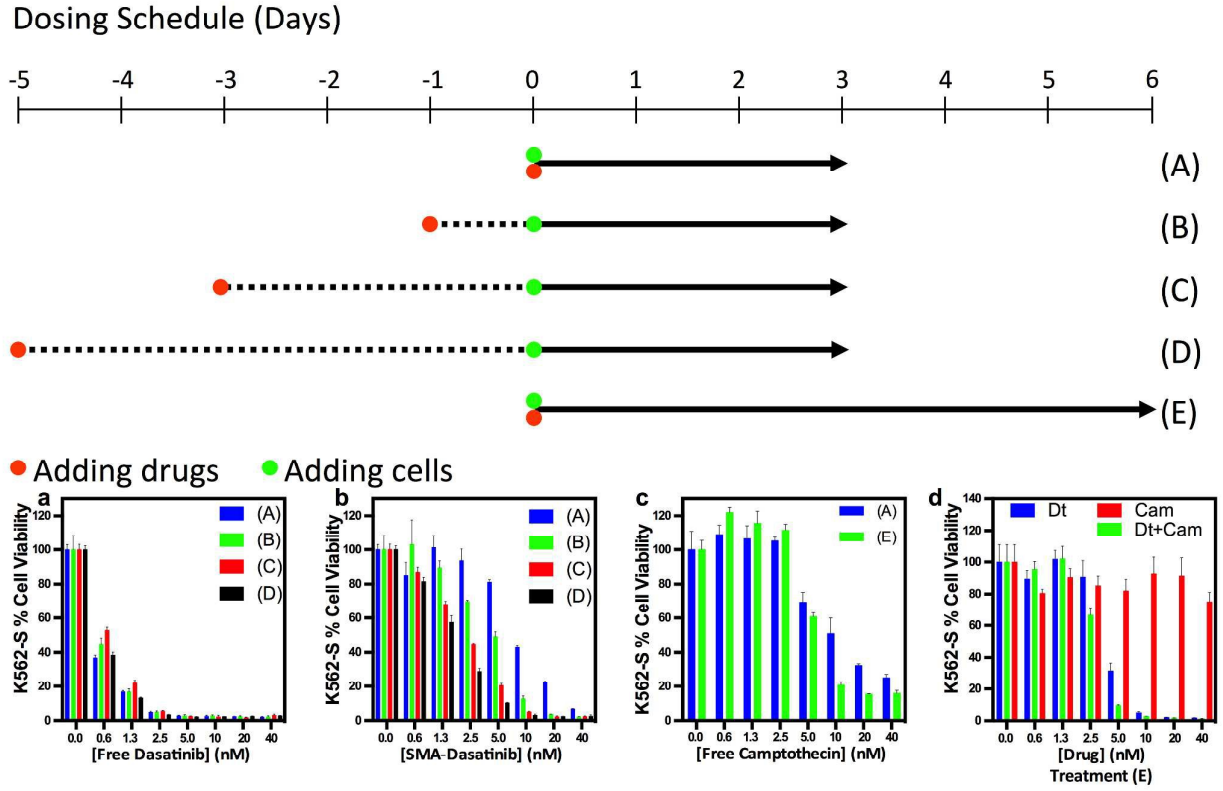

Fig. 4. Dosing scheme and cytotoxicity results for K562 cells incubated with poly(Cam-SMA-co-O950), poly(Dt-SMA-co-O950), and poly(Cam-SMA-co-O950-co-Dt-SMA) and free drug controls.

was synthesized. Here, a hydrophilic charge balanced macroCTA consisting of equimolar ratios of methacrylic acid and dimethylaminoethyl methacrylate (prepared from the copolymerization and subsequent TFA deprotection of tBMA and DMAEMA) was synthesized. Shown in Fig. 2a are the molecular weight chormatograms for the poly(tBMA-co-DMAEMA) macroCTA as well as the resultant poly(tBMA-co-DMAEMA)-b-(Dt-SMA) diblock copolymer. The high polymerization control imparted by the trithiocarbonate CTA can be seen by the narrow molecular weight distributions which clearly move to shorter elution times upon the addition of the second poly(Dt-SMA) block. Analysis of the ^{1}H NMR spectrum in DMSO-d_6 for the macroCTA indicate 51 and 49 mol % tBMA and DMAEMA residues which is in good agreement with the feed. Upon chain extension of this macroCTA with Dt-SMA, the ^{1}H NMR spectrum shows resonances associated with both block copolymer segments as well as the complete removal of the tertiary butyl ester protecting groups, which appears at 1.41 ppm (Fig. 2b).

Drug release studies in human serum

Drug release kinetics for the polymeric prodrugs were evaluated in 100 % human serum at 37 ^{o}C (Fig. 3a,b). Here, 33 ± 1.7 % of the Dt is released at 144 h relative to 22 ±1.4 % for Cam (Fig. 3a). These results suggest that the physiochemical properties of the linked drug play an important role in the drug release rates. As can be seen from Fig. 3b, the hydrolysis rates for the diblock copolymer, which self assembles into 43 nm particles under physiological pH and salt conditions, are substantially suppressed relative to the hydrophilic copolymers. Indeed 50 % Dt release was not observed until 384 h incubation with complete drug release not observed until approximately 50 days. Similar release profiles were observed for samples of the diblock copolymer incubated in human serum as well as low and high pH buffers. While the drug release profiles of the diblock copolymers are substantially slower than the analogous hydrophilic copolymers, they are capable of incorporating higher amounts of the prodrug residues into their structure (e.g. 44 wt. % Dt for the diblock copolymer employed in these studies). This combination of high drug loading and slow release profiles could be significant in drug delivery applications where a long lasting drug depot is desirable.

In vitro activity of poly(Dt-SMA-co-O950) and of poly(Dt-SMA-co-O950-co-CAM-SMA) in K562-S cells.

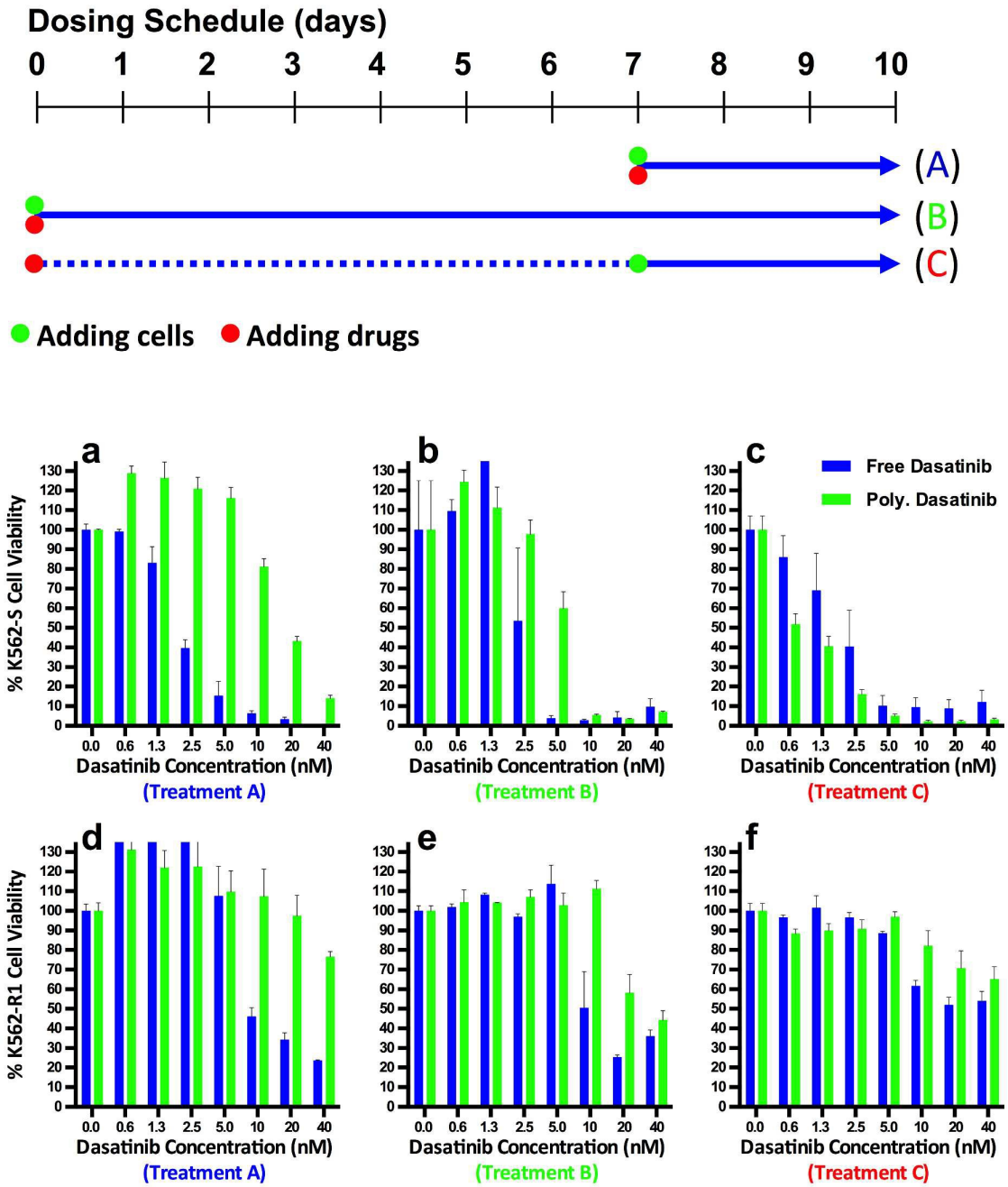

Fig. 5. Dosing scheme and cytotoxicity results for K562 and K562R cells incubated with poly[(DMAEMAcoMA)-b-(Dt-SMA)] and free drug controls.

The dosing schedules used to evaluate the polymeric prodrugs as well as the free drug controls are outlined in Fig. 4a-d. This dosing scheme was developed to evaluate the chemotherapeutic activity of the polymeric prodrugs under timeframes more closely reflecting those found *in vivo,* where the polymer-linked drugs may accumulate in tumor tissue. This enhanced accumulation of polymeric prodrugs within tumor tissue can occur via the enhanced permeation retention (EPR) effect.[37] The activities of free Dt as well as the polymeric prodrugs were tested in K562-S (immortalized human myelogenous leukemia) cells. As can be seen in Fig. 4a, K562-S cells are sensitive to free Dt with around 50 % cell viability observed at a drug concentration of 0.6 nM for all treatment regiments. There were no significant cytotoxicity differences between dosing schemes A through D, where free Dt is preincubated in 10 % Fetal bovine serum containing media at

37 °C for between 0 and 120 h prior to cell administration. This shows that the free drug is not degraded under these conditions. Based on this finding, the macromolecular prodrugs were preincubated according to this dosing scheme (Fig. 4b).

At an SMA-linked Dt concentration of between 1.25 and 10 nM a clear positive correlation between preincubation time and cytotoxic activity is observed. For example, a prodrug concentration of 5 nM preincubated for 0, 24, 72, and 120 hours result in 81, 49, 20, and 10 % cell viability respectively. The observed trend is consistent with drug release studies conducted in human serum (Fig. 3a), where the SMA-linked polymeric prodrug was shown to release 0, 5.6, 9.6 and 18.9 % of the ester linked drug at these time points. At prodrug concentrations above 10 nM, all dosing schemes resulted in nearly complete cell death while at prodrug concentrations below 1.25 nM low cytotoxic activity is observed. These findings suggest that the Dt conjugates are able to release the ester-linked drug in a controlled fashion while substantially increasing the aqueous solubility of the hydrophobic drug.

As highlighted in Scheme 1, chemotherapeutic copolymers can easily be prepared simply by copolymerizing the drug monomer with O950 at the desired molar feed ratio. In order to establish the ability of these constructs target multiple cytotoxic pathways, both Dt-SMA and Cam-SMA were copolymerized with O950 and then incubated with K562-S cells for either 72 or 144 h (no preincubation). As shown in Fig. 4c, free Cam is less cytotoxic to K562-S cells than Dt but still leads to high levels of cell death. At concentrations of 20 and 40 nM, 25 and 16 % cell viability were observed at 72 and 144 hours, respectively. In comparison, the SMA-linked Cam conjugates showed low cytotoxicity to these cells over the same period (Fig. 4d). Based on drug release studies (Fig. 3a), approximately 16 and 25 % of the covalently linked Cam is expected to be released at 72 and 144 hours respectively. These values yield a maximum Cam concentration of 6.4 and 10 nM respectively at the highest conjugate concentration. It also should be noted that cells incubated with free Cam receive the maximum drug dose over the entire treatment period while cells exposed to the conjugates experienced a tapered dose as the ester linkages hydrolyze. In contrast to the poly(Cam-SMA-co-O950) conjugate, high levels of chemotherapeutic activity are observed for both the poly(Dt-SMA-co-Cam-SMA-co-O950) and poly(Dt-SMA-co-O950) conjugates. These findings likely arise from a combination of higher intrinsic drug potency in these cells and increased hydrolysis rates of the SMA-linked Dt relative to the Cam derivatives.

Conjugates containing both Dt and Cam show a modest improvement in cytotoxicity relative to the Dt alone constructs (Fig. 4d). For example, at a Dt concentration of 5 nM both the poly(Dt-SMA-co-Cam-SMA-co-O950) and poly(Dt-SMA-co-O950) carriers show 28 and 43 % cell viability respectively following a 96 h incubation time. Under these conditions the poly(Dt-SMA-co-Cam-SMA-co-O950) treatment group also contains 5 nM Cam which seems to account for the additional 15 % reduction in cell viability relative to the Dt alone treatment. This effect is more substantial with the additional 21 % reduction at the 144 h treatment time where the same groups yield 31 and 10 % cell viability. While it isn't possible from the current studies to determine if the increase cytotoxicity is a synergistic or an additive effect these studies do demonstrates the ability of this system to incorporate multiple drug molecules into a single well-defined delivery system.

Determination of chemotherapeutic activity of poly(DMAEMA-co-MAA)-b-(Dt-SMA) in K562-S and K562-R1 cells.

The chemotherapeutic activity of a diblock copolymer-based Dt carrier, where the micellar core is made up of the hydrophobic drug monomer, was evaluated in Dt sensitive (K562-S) and resistant (K562-R1) cells (Fig. 5). As described above, separation of the hydrophobic Dt-SMA into a discrete hydrophobic segment results in a significant reduction in the drug release kinetics. For example, incubation of the diblock copolymer in human serum for 8 days yields only 30 % Dt release while the copolymer results in 45 % drug release over the same period. Despite this difference the diblock copolymer architecture may be advantageous in that it can carry higher quantities of the hydrophobic drug on a percent mass basis. The nanoparticle morphologies may also facilitate greater levels of cell uptake and favorable PK/biodistribution properties. The dosing schemes employed in these studies are outlined in Fig. 5. As expected, treatment of K562-S cells with free Dt results in near complete cell death at a drug concentration of at least 5 nM (Fig. 5a). It is interesting to note that even at the longest incubation period (10 days) only about 50 % of the indicated drug concentration is liberated from the polymer in an active form and yet similar cell viability levels are observed at the higher drug concentrations. This trend can be seen at 40 nM drug for dosing schemes B and C in both sensitive and resistant cells (Fig. 5b,c and e,f respectively). In the case of the K562-S cells, both the free drug and polymer conjugates showed comparable cytotoxicity at drug concentrations as low as 5 nM for dosing scheme C (Fig. 5c). The lack of a preincubation period shifts the minimum inhibitory concentration (MIC) of the conjugate to 10 nM for dosing scheme B relative to 5 nM for the free drug (Fig. 5b). As expected, dosing scheme A, where only around 13 % of the available drug is release over the entire incubation time, required higher conjugate concentrations to provide complete cell death (MIC ~ 40 nM). In contrast, incubation of Dt resistant K562-R1 cells at this concentration yields a negligible reduction in cell viability for all three dosing schemes investigated (Fig. 5d,e,f). Increasing the Dt concentration to 10 nM and above results in improved cytotoxicity for the free drug however even at 40 nM, 24 % cell viability is observed for treatment A. Longer incubation times resulted in cell recovery and increased proliferation. In comparison the polymer conjugates show relatively favorable cytotoxicity profiles in k562-R1 cells

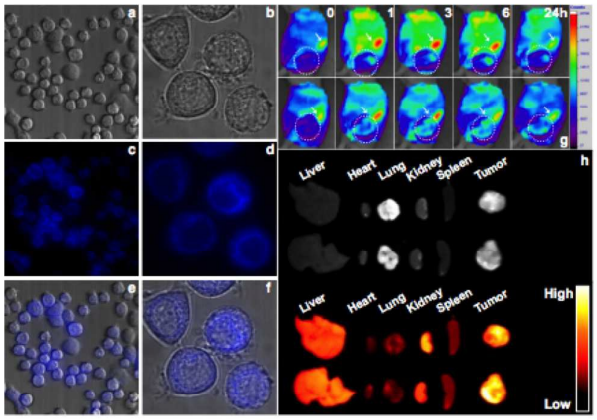

Fig. 6. Live cell fluorescence microscopy images of SKBR3 cells incubated for 1 hour with fluorescently labeled macromolecular prodrugs and in vivo imaging of alexafluor 647 labeled materials in mice bearing prostate tumor xenographs.

relative to the free drug for dosing schemes B and C, where there is sufficient time for some of the covalently linked drug to release, but unfavorably for dosing scheme A with a short incubation period (Fig. 5e,f). These results may be a result of enhanced uptake and retention of the nanoparticle prodrugs in K562-R1 cells relative to the free drug. These cells have been shown to express high level of efflux transport p-glycoprotein (Pgp) compared with K562-S.[38].

In vitro and in vivo imaging of the polymeric prodrugs

Live cell fluorescence microscopy was employed in order to visualize uptake and retention of labeled polymer conjugates (Fig. 6 a-d). In these studies, an adherent SKBR3 breast cancer cell line was incubated with the conjugates for 1 hour after which time the cells were washed with fresh media and subsequently imaged. The bright field and fluorescent images (at two magnifications) of the cells following treatment with the polymer conjugates are shown in Fig. 6a,b. From an overlay of these images (Fig. 6e,f) colocalization of the polymer fluorescence can be observed. This finding suggests that some portion of the macromolecular scaffold is internalized by 1 hour despite the nonionic hydrophilic character of the dense polyethylene glycol brush. Shown in Fig. 6g,h are the results of live animal imaging experiments conducted in mice bearing PC-3 (human prostate cancer cell line) tumor xenographs. In these studies, the polymer conjugates were labeled with Alexa Fluor 647 cadaverine. Fluorescent imaging of the tumor bearing mice immediately following administration of the macromolecular conjugates shows an initial accumulation of the polymers in the kidneys over the course of 6. By 24 hours post injection, this fluorescence was substantially reduced relative to earlier time points. In contrast the amount of fluorescence accumulating in the tumor tissue was observed to increase relative to initial values with substantial fluorescence retained even at 24 hours post injection. The increased accumulation of the fluorescently labeled conjugates in tumor tissue can be clearly visualized in ex vivo images (Fig. 6h). As can be seen in the fluorescent images, there is a significant amount of the polymeric prodrugs within the tumor tissue with progressively less fluorescence in the kidneys and liver respectively.

Conclusions

Polymeric prodrugs were prepared from the chemotherapeutic agents Cam and Dt via the direct RAFT polymerization of polymerizable prodrug monomers without the need for post-polymerization conjugation reactions. The covalently linked drugs were dispersed within hydrophilic polyethylene glycol methacrylate brushes or homopolymerized from a hydrophilic macroCTA to form a discrete polydrug segment. In all cases the copolymers were shown to have narrow molecular weight distributions and compositions comparable to the feed. The ester-linked prodrugs were shown to release the free drug via ester hydrolysis from the macromolecular scaffolds in human serum with rates dependent on both the physiochemical nature of the drug as well as the overall polymer morphology. Self-assembly of the diblock copolymers with a hydrophobic polydrug core was shown to significantly reduce drug release rate but also allowed for high drug loading densities. Live animal imaging in PC-3 (human prostate cancer cell line) tumor xenographs showed that the fluorescently labeled copolymer brushes were trafficked to the tumor 24 hours post injection. Ex vivo analysis of the harvested tissues showed that polymer accumulated preferentially in the tumor and kidneys. In vitro cytotoxicity measurements conducted in K562-S and K562-R cells demonstrated ability of the macromolecular conjugates to release the covalently linked drugs in an active form.

C Experimental

Materials

Chemicals and all materials were supplied by Sigma-Aldrich unless otherwise specified. Camptothecin and Dasatinib were purchased from VWR. Spectra/Por regenerated cellulose dialysis membranes (6-8 kDA cutoff) were obtained from Fisher Scientific. G-25 prepacked PD10 columns were obtained from GE Life Sciences. MTS cytotoxicity kits were obtained from Promega. Alexa Fluor 647 cadaverine, disodium salt was purchased from ThermoFisher. Tertiary butyl methacrylate (tBMA) was passed through a short plug of aluminum oxide (activated basic) to remove the inhibitor. Dimethylaminoethyl methacrylate (DMAEMA) was distilled under reduced pressure. 4-Cyano-4-(thiobenzoylthio)pentanoic acid (CTP) was obstained from Strem Chemicals inc. Ethyl cyanovaleric acid trithiocarbonate (ECT) was synthesized as described previously.[39] V40 and ABCVA were obtained from VWR and used as received. Liquid Sera Human from AB blood donor (US origin) was purchased from Sigma Aldrich (St. Louis, MO) and used as received.

Synthesis of N-(2-Chloro-6-methylphenyl)-2-[[6-[4-(2-methacryloxyethylsuccinylethyl)-1-piperazinyl)]-2-methyl-4-pyrimidinyl]amino)]-1,3-thiazole-5-carboxamide (Dt-SMA). To a mixture of 2-(methacryloyloxyethyl) monosuccinate (SMA) 920 mg (4 mmol) and N,N,N',N'-tetramethyl-O-(1*H*-benzotriazol-1-yl)uronium hexafluorophosphate (HBTU) 1.9 g (5 mmol) in 25 mL anhydrous DMF was added N,N-diisopropylethylamine 1.4 mL (8 mmol) at 0 ^{o}C. After 10 min. at 0 ^{o}C, the solution was stirred at room temperature for 20 min. *N*-(2-Chloro-6-methylphenyl)-2-[[6-[4-(2-hydroxyethyl)-1-piperazinyl)]-2-methyl-4-pyrimidinyl]amino)]-1,3-thiazole-5-carboxamide 976 mg (2 mmol) was then introduced as solid, and stirring was continued at room temperature for 6 h. The reaction mixture was poured into ice cold water and stirred for 20 min. The off-white solid obtained was filtered, washed with water and dried under high vacuum. The crude ester was dissolved in 15 mL of 15 % methanol in chloroform and purified by column chromatography using 10 % methanol in chloroform containing 0.3 % NH_4OH. Yield = 990 mg (70.7 %). ^{1}H NMR (300 MHz, DMSO-d_6, ppm) δ 11.46 (s, 1H, **H14**), 9.87 (s, 1H, **H16**), 8.20 (s, 1H, **H13**), 7.38 (d, *J* = 6.2 Hz,1H, **H20**), 7.31-7.18 (m, 2H, **H18 & H19**), 6.08-5.97 (m, 2H, **H2 & H15**), 5.58 (s, 1H, **H1**), 4.27 (s, 4H, **H4 & H5**), 4.13 (t, *J* = 5.7 Hz, 2H, **H8**), 3.49 (s, 4H, **H11**), 2.63-2.52 (m, 6H, **H9 & H10**), 2.48 (m, 4H, **H6 & H7** merged with DMSO peak), 2.39 (s, 3H, **H12**), 2.22 (s, 3H, **H17**), 1.85 (s, 3H, **H3**); ^{13}C NMR (125 MHz, DMSO-d_6, ppm) δ 172.3, 166.9, 165.6, 163.1, 162.8, 160.4, 157.4, 141.3, 139.3, 136.1, 134.0, 132.9, 129.5, 128.6, 127.5, 126.6, 126.2, 83.1, 62.9, 62.5, 62.0, 56.4, 52.8, 44.0, 29.08, 29.05, 26.0, 18.8, 18.4; ESI-MS ($C_{32}H_{38}ClN_7O_7S$): *m/z* = 701.0 $[M+1]^+$ and 722.5 $[M+Na]^+$.

Synthesis of Cam-SMA. To a solution of mono-2-(methacryloyloxy)ethyl succinate (SMA) was added 460 mg (2 mmol), *N*-(3-dimethylaminopropyl)-*N'*-ethylcarbodimide hydrochloride (EDCI.HCl) 767 mg (4 mmol) and N,N-dimethylpyridin-4-amine (DMAP) 122 mg (1 mmol) in 60 mL CH_2Cl_2 was added camptothecin 348 mg (1 mmol) as solid. After stirring at RT for 6 h, the reaction mixture was washed with water (2 X 30mL) and the organic phase was dried over anhydrous sodium sulfate. After evaporation of the solvent under reduced pressure, the resulting crude product was purified by silica gel column chromatography using 7 % methanol in chloroform. Yield = 544 mg (97.0 %). ^{1}H NMR (300 MHz, $CDCl_3$, ppm): δ 8.39 (s, 1H, **H13**), 8.23 (d, *J* = 8.4 Hz, 1H, **H17**), 7.94 (d, *J* = 8.1 Hz, 1H, **H14**), 7.83 (t, *J* = 7.6 Hz, 1H, **H15**), 7.67 (t, *J* = 7.5 Hz, 1H, **H16**), 7.29 (s, 1H, **H11**), 6.06 (s, 1H, **H1**), 5.67 (d, *J* = 17.2 Hz,1H, **H10**), 5.55 (s, 1H, **H2**), 5.39 (d, *J* = 17.2 Hz,1H, **H10**), 5.28 (s, 1H, **H12**), 4.20 – 4.40 (m, 4H, **H4 & H5**), 2.85 (m, 2H, **H7**), 2.70 (m, 2H, **H6**), 2.06-2.39 (m, 2H, **H8**), 1.89 (s, 3H, **H3**), 0.99 (t, *J* = 7.4 Hz, 3H, **H9**); ^{13}C NMR (125 MHz, DMSO-d_6, ppm) δ 171.5, 171.2, 167.3, 167.0, 157.3, 152.3, 148.8, 146.2, 145.9, 135.8, 131.2, 130.7, 129.5, 128.5, 128.2, 128.1, 128.0, 126.0, 120, 96.2, 76.3, 67.0, 62.5, 62.2, 49.9, 31.8, 28.9, 28.7, 18.2, 7.60. ESI-MS ($C_{30}H_{28}N_2O_9$): *m/z* = 561.9 $[M+1]^+$, 583.5 $[M+Na]^+$ and 599.3 $[M+K]^+$.

Synthesis of poly(Cam-SMA-co-O950). Copolymerization of Cam-SMA and O950 was conducted in DMSO at 70 ^{o}C for 18 h in the presence of CTP and ABCVA. The initial molar feed percentages of the Cam-SMA and O950 monomers were both 50 %. The $[M]_o$:$[CTA]_o$:$[I]_o$) was 25:1:0.1 at an initial monomer concentration of 20 wt. %. To a 10 mL round bottom flask was added Cam-SMA (0.433 g , 0.772 mmol), O950 (0.733 g, 0.772 mmol), CTP (17.2 mg, 0.062 mmol), ABCVA (1.73 mg, 0.0062 mmol), and DMSO (4.66 mL). The round bottom flask was then sealed with a rubber septa and purged with nitrogen for 1 hour. After this time the polymerization solution was transferred to a preheated water bath at 70 ^{o}C and allowed to react for 18 hours. After this time the solution was precipitated into a 50 times excess of diethyl ether. The precipitate was then redissolved in minimal acetone and then precipitated once more into diethyl ether. This process was repeated five additional times after which the copolymer was dried under high vacuum for 48 hours. The dry polymer was then further purified via sephadex PD10 column according to the manufactures instructions. The final copolymer was subsequently isolated by lyophilization. Copolymer composition was determined to be 53 % O950 and 47 % Cam-SMA by integrating the combined ester resonances between 3.7 and 4.5 ppm (4H Cam-SMA + 2H O950) (X) to the Cam-SMA resonances between 4.7 and 5.7 ppm (4H Cam-SMA) (Y) using the equation ^{1}H Cam-SMA = Y/4 and ^{1}H O950 = (X-Y)/2. SEC analysis yielded M_n and Đ of 26 500 and 1.16 respectively.

Synthesis of poly(Dt-SMA-co-O950). Copolymerization of Dt-SMA and O950 was conducted in DMSO at 70 ^{o}C for 18 h in the presence of CTP and ABCVA. The initial molar feed percentages of the Dt-SMA and O950 monomers were both 50 %. The $[M]_o$:$[CTA]_o$:$[I]_o$) was 25:1:0.1 at an initial monomer concentration of 20 wt. %. To a 10 mL round bottom flask was added Dt-SMA (0.300 g, 0.428 mmol), O950 (0.407 g, 0.428 mmol), CTP (9.58 mg, 0.034 mmol), ABCVA (0.96 mg, 0.0034 mmol), and DMSO (2.83 mL). The round bottom flask was then sealed with a rubber septa and purged with nitrogen for 1 hour. After this time the polymerization solution was transferred to a preheated water bath at 70 ^{o}C and allowed to react for 18 hours. After this time the solution was precipitated into a 50 times excess of diethyl ether. The precipitate was then redissolved in minimal acetone and then precipitated once more into diethyl ether. This process was repeated five additional times after which the copolymer was dried under high vacuum for 48 hours. The dry polymer was then further purified via sephadex PD10 column according to the manufactures instructions. The final copolymer was subsequently isolated by lyophilization. Copolymer composition was determined to be 46 % O950 and 54 % Dt-SMA by integrating the combined resonances between 3.7 and 4.5 ppm (6H Dt-SMA + 2H O950) (X) to the Dt-SMA resonance between 5.9 and 6.1 ppm (1H Dt-SMA) (Y) using the equation ^{1}H Dt-SMA = Y and ^{1}H O950 = (X-6Y)/2. SEC analysis yielded M_n and Đ of 28 000 and 1.10 respectively.

Synthesis of poly(Cam-SMA-co-Dt-SMA-co-O950). Copolymerization of Dt-SMA, Cam-SMA, and O950 was conducted in DMSO at 70 ^{o}C for 18 h in the presence of CTP and ABCVA. The initial molar feed percentages of Cam-SMA, Dt-SMA and O950 were 25, 25 and 50 mol % respectively. The $[M]_o$:$[CTA]_o$:$[I]_o$) was 25:1:0.2 at an initial monomer concentration of 20 wt. %. To a 10 mL round bottom flask was added Cam-SMA (0.120 g, 0.214 mmol), Dt-SMA (0.150 g, 0.214 mmol), O950 (0.407 g, 0.428 mmol), CTP (9.57 mg, 0.034 mmol), ABCVA (1.92 mg, 0.0069 mmol), and DMSO (2.71 mL). The round bottom flask was then sealed with a rubber septa and purged with nitrogen for 1 hour. After this time the polymerization solution was transferred to a preheated water bath at 70 ^{o}C and allowed to react for 18 hours. After this time the solution was precipitated into a 50 times excess of diethyl ether. The precipitate was then redissolved in minimal acetone and then precipitated once more into diethyl ether. This process was repeated five additional times after which the copolymer was dried under high vacuum for 48 hours. The dry polymer was then further purified via sephadex PD10 column according to the manufactures instructions. The final copolymer was subsequently isolated by lyophilization. Copolymer composition was determined to be 49 mol % O950, 24 mol % Cam-SMA, and 27 mol % Dt-SMA respectively by integrating the combined resonances ester between 3.8 and 4.5 ppm (4H Cam-SMA, 2H O950, 6H Dt-SMA) (X), the Dt-SMA resonances 5.9 between 6.1 and ppm (1H Dt-SMA) (Y), and the Cam-SMA resonances between 4.7 and 5.7 ppm (4H Cam-SMA) (Z) using the equation: ^{1}H Dt-SMA = X, ^{1}H Cam-SMA = Z/4 and ^{1}H O950 = (Y-X*6-Y)/2. SEC analysis yielded M_n and Đ of 29 000 and 1.19 respectively.

Synthesis of poly(tBMA-co-DMAEMA). The copolymerization of tBMA and DMAEMA was conducted in dioxane at 90 ^{o}C for 5 h in the presence of ECT and V40 as the RAFT agent and radical initiator respectively with an equimolar initial molar feed ratio of tBMA and DMAEMA. The $[M]_o$:$[CTA]_o$:$[I]_o$) was 60:1:0.05 at an initial monomer concentration of 50 wt. %. To a 100 mL round bottom flask was added DMAEMA (20 g, 0.127 mol), tBMA (18.09 g, 0.127 mol), ECT (1.11 g, 4.22 mmol), V40 (51.6 mg, 0.211 mmol), and dioxane (38 mL). The round bottom flask was then sealed with a rubber septa and purged with nitrogen for 1 hour. After this time the polymerization solution was transferred to a preheated water bath at 90 ^{o}C and allowed to react for 5 hours. After this time the solution transferred to a spectrapor regenerated cellulose dialysis membrane (6-8 kDa cutoff) and dialyzed against acetone at 5 ^{o}C. After three changes of the acetone the copolymer was then furthered dialyzed against water at which point it precipitated. The resultant precipitate was collected and lyophilized under high vacuum. Copolymer composition was determined by comparing the combined backbone region to the DMAEMA ester resonance.

Synthesis of poly[(MA-co-DMAEMA)-b-(Dt-SMA)]. Polymerization of Dt-SMA from a poly(tBMA-co-DMAEMA) macroCTA was conducted in DMSO at 70 ^{o}C for 18 hours. The $[M]_o$:$[CTA]_o$:$[I]_o$) was 12.5:1:0.02 at an initial monomer concentration of 20 wt. %. To a 5 mL round bottom flask was added Dt-SMA (0.380 g, 0.542 mmol), poly(tBMA-co-DMAEMA) macroCTA (0.260 g, 0.0434 mmol) ABCVA (2.43 mg, 0.0087 mmol), and DMSO (1.78 mL). The round bottom flask was then sealed with a rubber septa and purged with nitrogen for 30 minutes. After this time the polymerization solution was transferred to a preheated water bath at 70 ^{o}C and allowed to react for 18 hours. After this time the solution was precipitated into a 20 times excess of diethyl ether from DMSO (x5). The tertiary butyl ester groups were subsequently removed by dissolving the polymer in neat TFA at a concentration of 5 wt % for 8 hours. The polymer was then isolated by precipitation into ether followed by neutralization by dialysis against PBS (0.20 M) at 5 ^{o}C followed by water. The diblock copolymer was then further purified using a PD10 desalting column according to the manufactures instructions. The final copolymer composition was determined as shown in Fig. 2b.

Cell culture and cytotoxicity measurements. K562-S (Imatinib sensitive cells) and K562-R1 (Imatinib resistant cells) cells were cultured in RPMI 1640 (Gibco) supplemented with 10% fetal bovine serum (FBS), 100 U/ml penicillin, and 100 µg/ml streptomycin (Gibco) in a 37°C, 5% CO_2 incubator. Note: K562-r cells do not have mutations in the ABL tyrosine kinase domain that would confer resistance. Resistance has been postulated to result from increases in LYN kinases as well as drug efflux.[40] Free drugs and campothecin/Dt polymers were preincubated with culture media containing 10 % FBS for 0 day, 1 day, 3 days, and 5 days at a 37°C, 5% CO_2 incubator before cell seeding. K562-S and K562-R1 cells were suspended with culture media containing 10 % FBS and 5 X 10^3 cells/well were seeded and treated with increasing concentrations of the preincubated drugs in a 96-well plate (Costar). After 3 days or 6 days, for measuring the results of cell viability, the MTS reagent (Promega) was added in a final concentration of 317 µg/ml in the assay wells. After incubation for 1 hr, the absorbance at 490 nm was measured by a 96-well plate reader. The cell viability of treated cells were determined upon normalizing to the cell viability of non-treatment.

GPC chromatography. Absolute molecular weights and molar mass dispersities were determined using using Tosoh SEC TSK-GEL α-3000 and α-e4000 columns (Tosoh Bioscience, Montgomeryville, PA) connected in series to an Agilent 1200 Series Liquid Chromatography System (Santa Clara, CA) and Wyatt Technology miniDAWN TREOS, 3 angle MALS light scattering instrument and Optilab TrEX, refractive index detector (Santa Barbara, CA). HPLC-grade DMF containing 0.1 wt.% LiBr at 60 ^{o}C was used as the mobile phase at a flow rate of 1 mL/min.

Analysis of drug release by High-performance Liquid Chromatography. The HPLC analysis of drug release was carried out with an Agilent 1260 Quaternary HPLC Pump, Agilent 1260 Infinity Standard Automatic Sampler, Agilent

1260 Infinity Programmable Absorbance Detector, and Agilent ChemStation software for LC system (Palo Alto, CA). Dt, Cam, and liquid human serum from AB blood donor were used as received. The analyte was separated at ambient temperature using a Zorbax RX-C_{18} (4.6 x 150 mm; 5 µm) analytical column (Agilent Technologies, CA).

Analysis of Dt was conducted at 325 nm with a mobile phase consisting of 2% aqueous acetic acid and acetonitrile (84:16) v/v. The flow rate was set at 1.0 mL/min and sample injection volume at 20 µL. A stock solution of Dt was prepared in deionized water at 10 mg/mL. Working solutions of Dt for standard curves were diluted from stock solution using the mobile phase to the listed concentrations of 300 µg/mL, 200 µg/mL, 100 µg/mL, 50 µg/mL, 25 µg/mL, 12.5 µg/mL, 6.25 µg/mL, and 3.12 µg/mL. These solutions were then diluted with a 1:1 v/v ratio of either mobile phase:deionized water or mobile phase:human serum to create final Dt standards of 150 µg/mL, 100 µg/mL, 50 µg/mL, 25 µg/mL, 12.5 µg/mL, 6.25 µg/mL, and 3.12 µg/mL for pharmaceutical and biological analysis, respectively. Both non-serum (mobile phase:deionized water) and serum standards were subsequently treated with 50% acetonitrile (v/v) to promote protein precipitation. Serum standards were centrifuged at 12,000g for 15 minutes and supernatants were collected and filtered using a 0.45µm low protein-binding filter before running on the HPLC. Non-serum standards were run without the need for centrifugation. All standards were processed using a gradient HPLC elution profile for 15 minutes followed by 10 minutes of column washing with acetonitrile and water and 5 minutes of equilibration with mobile phase.

Cam release from polymer conjugates was carried out in serum and buffer (150 mM pH 7.4 sodium phosphate, 150 mM pH 5.8 sodium acetate) at 37 ˚C at a polymer concentration of 6 mg/mL. Quantification of total Cam in polymer conjugates was measured by taking 6 mg/mL of polymer in 10% aq. H_2SO_4 for 72 h at 25 ˚C. The HPLC with a gradient elution profile was used to quantify amount of drug released using the same instrument parameters set forth for drug standards. A 1:1 dilution of serum or buffer samples with methanol:water (75:25) v/v was conducted, followed by another 1:1 dilution with acetonitrile. The resulting samples were vortexed and centrifuged at 12,000g for 15 minutes. Supernatants were collected and filtered using a 0.45µm low protein binding filter before HPLC analysis at 370 nm. Percent (%) drug released was subsequently quantified using the formula: % Drug Released = [Peak(t_x) – Peak(t_0)]/[Peak(H_2SO_4)], where t_x and t_0 are the peaks resolved by the HPLC at time x and zero, respectively, and Peak(H_2SO_4) denotes total drug present in the polymer system.

Acknowledgements

This work was funded by the National Institutes of Health (grants R01EB002991 and 1R21EB014572-01A1), Global Innovative Research Center (GiRC) project (2012K1A1A2A01056095) of National Research Foundation of Korea, and Intramural Research Program of KIST.

Notes and References

1 A. Paci, G. Veal, C. Bardin, D. Levêque, N. Widmer, J. Beijnen, A. Astier and E. Chatelut, *European Journal of Cancer*, 2014, **50**, 2010–2019.
2 I. F. Tannock, C. M. Lee, J. K. Tunggal, D. S. M. Cowan and M. J. Egorin, *Clin Cancer Res*, 2002, **8**, 878–884.
3 H. Chen, C. Khemtong, X. Yang, X. Chang and J. Gao, *Drug Discovery Today*, 2011, **16**, 354–360.
4 D. D. Lasic, *Journal of Controlled Release*, 1997, **48**, 203–222.
5 M. E. R. O'Brien, N. Wigler, M. Inbar, R. Rosso, E. Grischke, A. Santoro, R. Catane, D. G. Kieback, P. Tomczak, S. P. Ackland, F. Orlandi, L. Mellars, L. Alland, C. TendlerCAELYX Breast Cancer Study Group, *Ann. Oncol.*, 2004, **15**, 440–449.
6 T. M. Allen and P. R. Cullis, *Advanced Drug Delivery Reviews*, 2013, **65**, 36–48.
7 K. Cho, X. Wang, S. Nie, Z. G. Chen and D. M. Shin, *Clin Cancer Res*, 2008, **14**, 1310–1316.
8 M. E. Davis, Z. G. Chen and D. M. Shin, *Nat Rev Drug Discov*, 2008, **7**, 771–782.
9 R. K. Jain and T. Stylianopoulos, *Nat Rev Clin Oncol*, 2010, **7**, 653–664.
10 E. Miele, G. P. Spinelli, E. Miele, F. Tomao and S. Tomao, *International Journal of Nanomedicine*, 2009, **4**, 99–105.
11 L. W. Seymour, K. Ulbrich, J. Strohalm, J. Kopecek and R. Duncan, *Biochemical Pharmacology*, 1990, **39**, 1125–1131.
12 J. Kopecek, P. Rejmanová, R. Duncan and J. B. Lloyd, *Ann. N. Y. Acad. Sci.*, 1985, **446**, 93–104.
13 Z.-H. Peng and J. Kopeček, *J. Am. Chem. Soc.*, 2015, **137**, 6726–6729.
14 J. Kopecek, P. Kopečková, T. Minko, Z. R. Lu and C. M. Peterson, *Journal of Controlled Release*, 2001, **74**, 147–158.
15 J. Yang, R. Zhang, D. C. Radford and J. Kopeček, *J Control Release*, 2015, **218**, 36–44.
16 S. Eliasof, D. Lazarus, C. G. Peters, R. I. Case, R. O. Cole, J. Hwang, T. Schluep, J. Chao, J. Lin, Y. Yen, H. Han, D. T. Wiley, J. E. Zuckerman and M. E. Davis, *PNAS*, 2013, **110**, 15127–15132.
17 Jianjun Cheng, Kay T Khin, Gregory S Jensen, A. Aijie LiuMark E Davis, *Bioconjugate Chemistry*, 2003.
18 H. Han and M. E. Davis, *Mol. Pharm.*, 2013, **10**, 2558–2567.
19 M. C. Parrott, M. Finniss, J. C. Luft, A. Pandya, A. Gullapalli, M. E. Napier and J. M. DeSimone, *JACS*, 2012.
20 C. Boyer, V. Bulmus, T. P. Davis, V. Ladmiral, J. Liu and S. Perrier, *Chemical Reviews*, 2009, **109**, 5402–5436.
21 J. Chiefari, Y. K. Chong, F. Ercole, J. Krstina, J. Jeffery, T. P. T. Le, R. T. A. Mayadunne, G. F. Meijs, C. L. Moad, G. Moad, E. Rizzardo and S. H. Thang, *Biomacromolecules*, 1998, 5559–5562.
22 K. Matyjaszewski and J. Xia, *Chemical reviews*, 2001, **101**, 2921–2990.
23 X. Chen, S. McRae, S. Parelkar and T. Emrick, *Bioconjugate chemistry*, 2009, **20**, 2331–2341.
24 H. Wei, C. E. Wang, N. Tan, A. J. Boydston and S. H. Pun, *Submitted*, 2015.
25 D. D. Lane, D. Y. Chiu, F. Y. Su, S. Srinivasan, H. B. Kern, O. W. Press, P. S. Stayton and A. J. Convertine, *Polym. Chem.*, 2014.

26 A. X. Gao, L. Liao and J. A. Johnson, *Macro Letters*, 2014, **3**, 854–857.
27 X. Li, Y. Qian, T. Liu, X. Hu, G. Zhang, Y. You and S. Liu, *Biomaterials*, 2011, **32**, 6595–6605.
28 J. A. Johnson, Y. Y. Lu, A. O. Burts, Y. Xia, A. C. Durrell, D. A. Tirrell and R. H. Grubbs, *Macromolecules*, 2010, **43**, 10326–10335.
29 J. A. Johnson, Y. Y. Lu, A. O. Burts, Y.-H. Lim, M. G. Finn, J. T. Koberstein, N. J. Turro, D. A. Tirrell and R. H. Grubbs, *J. Am. Chem. Soc.*, 2011, **133**, 559–566.
30 D. D. Lane, D. Y. Chiu, F. Y. Su, S. Srinivasan, H. B. Kern, O. W. Press, P. S. Stayton and A. J. Convertine, *Polymer Chemistry*, 2015, **6**, 1286–1299.
31 M. B. L. Kryger, A. A. A. Smith, B. M. Wohl and A. N. Zelikin, *Macromolecular Bioscience*, 2014, **14**, 173–185.
32 M. B. L. Kryger, B. M. Wohl, A. A. A. Smith and A. N. Zelikin, *Chemical Communications*, 2013, **49**, 2643–2645.
33 D. Das, S. Srinivasan, A. M. Kelly, D. Y. Chiu, B. K. Daugherty, D. M. Ratner, P. S. Stayton and A. J. Convertine, *Polymer Chemistry*, 2016.
34 D. Roy, G. Y. Berguig, B. Ghosn, D. D. Lane, S. Braswell, P. S. Stayton and A. J. Convertine, *Polymer Chemistry*, 2014, **5**, 1791–1799.
35 G. Y. Berguig, A. J. Convertine, S. Frayo, H. B. Kern, E. Procko, D. Roy, S. Srinivasan, D. H. Margineantu, G. Booth, M. C. Palanca-Wessels, D. Baker, D. Hockenbery, O. W. Press and P. S. Stayton, *Molecular Therapy*, 2015, 1–11.
36 D. Roy, G. Y. Berguig, B. Ghosn, D. D. Lane, S. Braswell, P. S. Stayton and A. J. Convertine, *Polymer Chemistry*, 2014.
37 A. K. Iyer, G. Khaled, J. Fang and H. Maeda, *Drug Discovery Today*, 2006, **11**, 812–818.
38 J. Klawitter, D. J. Kominsky, J. L. Brown, J. Klawitter, U. Christians, D. Leibfritz, J. V. Melo, S. G. Eckhardt and N. J. Serkova, *British Journal of Pharmacology*, 2009, **158**, 588–600.
39 A. J. Convertine, D. S. W. Benoit, C. L. Duvall, A. S. Hoffman and P. S. Stayton, *Journal of Controlled Release*, 2009, **133**, 221–229.
40 M. Dufies, A. Jacquel, N. Belhacene, G. Robert, T. Cluzeau, F. Luciano, J. P. Cassuto, S. Raynaud and P. Auberger, *Oncotarget*, 2011, **2**, 874–885.